

# Three-Dimensional Stratigraphy View from Ground Penetrating Radar Attributes for Soil Characterization



Amalina Yusof, Muhamad Mubiin Abdul Manas,  
Zulkarnaini Mat Amin and Nurhazimah Husna Shokri

**Abstract** The Ground Penetrating Radar (GPR), a geophysical technique that uses non-destructive testing to detect objects and structure beneath the soil was a huge contribution in survey and engineering, especially in underground utility. GPR has been used since 1970 and the method is still undergoing upgrade alongside the sophisticated processing software. Nevertheless, soil is the principal medium which interferes with the signal penetration of GPR due to its physical and electrical properties. Thus, a study using soil stratigraphy is a prerequisite to understanding GPR radargram. In this study, a test bed was constructed to simulate different soil layers which consist of existing clay, sand, small stone, and crusher run stone. The GPR instrument with frequencies of 100, 250, 400, 750, and 900 MHz was used to collect the data. The processing was carried out using reflex software for image interpretation and three-dimensional (3D) visualizations. This study is expected to help surveyors in understanding the measurement, for example, soil composition, problems related to GPR underground surveying.

**Keywords** Three dimensional · Stratigraphy · Ground penetrating radar

## 1 Introduction

Malaysia is currently undergoing profound development and construction with an extensive underground utility installation such as for water reticulation, sewerage, electric, gas, and telephone [1, 2]. Thus, information on a particular location of utility installation is necessary to decrease any disturbance that would result in

---

A. Yusof · M. M. A. Manas · Z. M. Amin (✉) · N. H. Shokri  
Geomatic Innovation Research Group, Faculty of Geoinformation  
and Real Estate, Universiti Teknologi Malaysia, 81310 Skudai,  
Johor, Malaysia  
e-mail: zulkarnaini@utm.my

A. Yusof  
e-mail: amalinayusup@gmail.com

property damages, design changes, service breakdown, and business disruption or even cause injuries [3].

Due to the capability of subsurface imaging and user-friendly features, Ground Penetrating Radar (GPR) is used in many engineering works such as civil engineering [4–6], archaeology [7–10], forensics [11–13], earth sciences [14], military, and environmental studies [15]. This underground utility mapping uses the principle of geophysics to detect, identify, and investigate subsurface object buried in the ground [6].

An object could be identified whether it is buried in shallow or deeper depths based on the correct radar antenna frequency [16]. As the technology develops, GPR had been featured in wide applications for the last 40 years with a continuously upgraded software to facilitate better results [17].

GPR has become a very important tool for non-destructive testing for underground exploration. In fact, it is capable to produce high-resolution images of the shallow subsurface and underground utilities. However, one of the obstacles in getting such information would revolve around the type of the soil [18]. Therefore, this study would like to identify the properties of the soil for better GPR image resolution.

Soil is an assemblage isolated unit of earth's layer deposit which includes mineral composition or organic source occasionally. Soil properties and characteristics could be identified from the GPR imaging data. The performance of GPR helps to differentiate types of soils [19, 20]. Therefore, the soil profile data and information could be collected. However, different soil and moisture condition affect the efficiency performance of GPR [21].

Various types of soils make the ground itself contain a number of soil layers. The stratigraphy of soil gives information of the soil profile, whereby measurement and study of the soil profile could be done by measuring the thickness of certain soil layer [22, 23]. Moreover, stratigraphic information is very useful for visualization of sedimentary structures, sand body geometry, and stratigraphic architecture [24, 25]. In that case, the visualization of stratigraphic structure could be upgraded to 3D visualization for better evaluation.

Lately, 3D model mapping has been used in the surveying field. Most of the maps, nowadays, are produced in 3D form which contain more details than two-dimensional (2D) maps. 3D map shows more details on the surface of the earth, as well as below the earth surface.

There are many benefits of the 3D view compared to 2D view. First, 3D view allows a concise picture of an object for higher resolution. Yet, the versatility allows users to easily understand the information given. Furthermore, 3D view enables instant calculations and interpolation such as coordinate computation and provide information of soil stratigraphy in order to correlate the soil strata [26]. The GPR data is analysed by using software to create and view 3D stratigraphy [27]. Therefore, 3D stratigraphy view gives more information than old existing stratigraphy view.

## 2 Methodology

### 2.1 Test Bed Simulation

The test bed is constructed at a selected site as shown in Fig. 1. The site is located at the Universiti Teknologi Malaysia cluster area and marked with a red flag. The test bed is built as a simulation for the imaging of soil stratigraphy. For this simulation, the test bed is built with a dimension of 2 m length  $\times$  1 m wide  $\times$  1.2 m depth. In order to create various types of soil layers, certain types of soil were selected such as smooth sand, small granite stone, and crusher run stone.

The test bed was divided into three layers. The deepest layer is the smooth sand followed by small granite stone, and crusher run stone. These entire layers are perfectly divided into same depth, 0.4 m, with the same dimension in length and width.

After the test bed is filled up with these soils, the soil then was compacted by using a compactor machine. The best common means for soil stabilization to meet the recommended road scheme necessity is through compaction. Soil compaction is used to compress the soil to the ground by eliminating the air voids, pore spaces between soil particles. Additionally, soil compaction is a recommended method to reduce error as the air gap between the soils becomes smaller. Therefore, the errors of radar images could be reduced. Figure 2 shows the three layers of the constructed test bed.

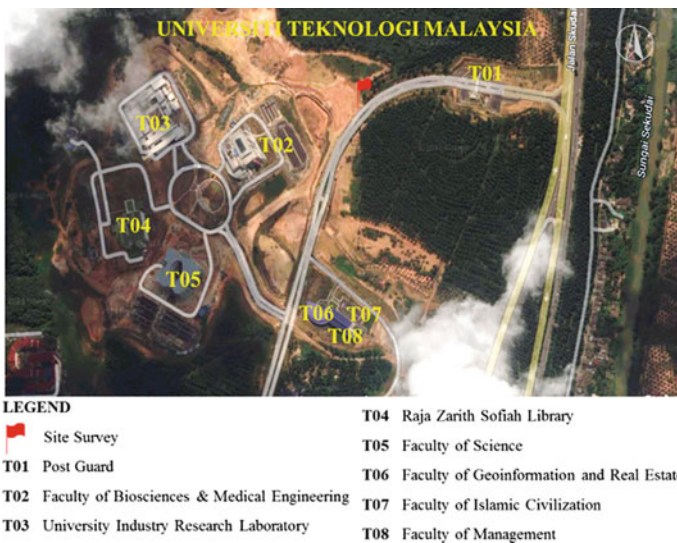
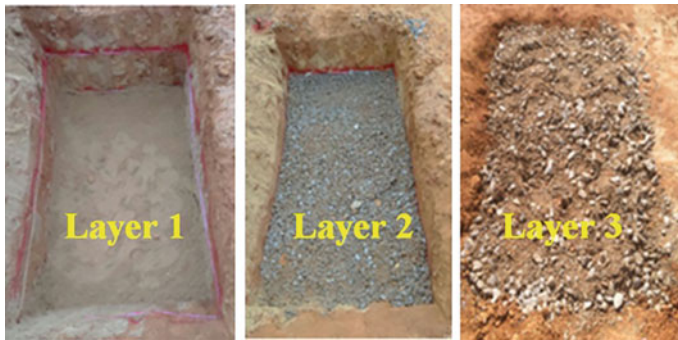


Fig. 1 Simulation site



**Fig. 2** Soil layers of the constructed test bed; layer 1 is the smooth sand, layer 2 is the small granite stone, and layer 3 is the crusher run stone

Data collection had been done by using GPR equipment with a variety of signal frequencies. The signal frequencies that had been used were 100, 250, 400, 750, and 900 MHz.

The extraction of the stratigraphy shows different resolution for different frequency. The low frequency creates a poor resolution, whereas the high frequency produces good resolution [28]. Hence, moderate frequency would best be employed.

The data collection surveys were performed by gridding method. It is commonly used to establish rectangular grids with 1 m or less line spacing, with interval of 0.5 m in this method [29–31]. The gridding sizes covered 3 m × 2 m area.

## 2.2 Data Processing

As for the data processing, the data underwent various stages before being presented as useful information. These stages include generalization, computation, adjustment, image filtering, and interpretation of raw radar data which validate the quality of the collected data. Then, the data is generated into 3D view. The software used to process this data is called Reflex2D and Reflex3D software. The result and analysis of the study is discussed in the next section.

## 3 Result and Discussion

### 3.1 Extraction of the Stratigraphy

The extraction of stratigraphy from the GPR images needs to be carried out according to several steps. The extraction of the stratigraphy is conducted by using

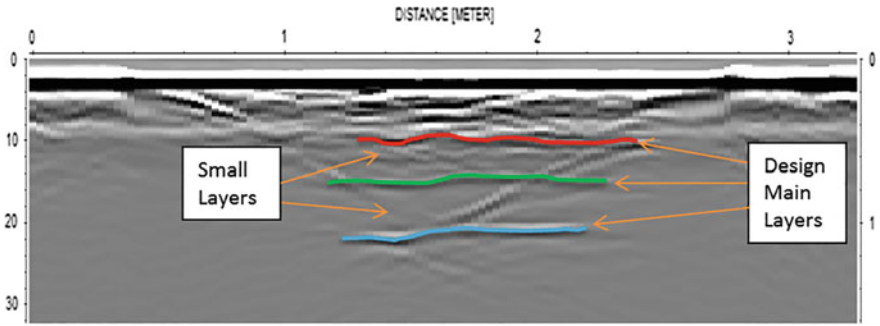


Fig. 3 Design of main soil layers on the radar image

Reflex2D software. In order to rectify and reduce errors, image filtering was employed. This software was used to process and identify the soil layers.

Then, the basic understanding of radar image interpretation is that the radar image would partially show the separation of the soil. Due to some blunders, the image would show more small layers than what exactly the soil layer has. This is because the signal from the radar would reflect when it encounters different mediums. The signal detects too many different changes of conductivities and velocity. As a result, the best way to solve this problem is to design the main layers of the soil. Figure 3 shows a radar image with the design of the main soil layers. The soil layers stratigraphy were then extracted from the radar images.

Next, it is possible to identify and extract the soil stratigraphy based on their reflection velocity from the radargram. From the radargram, the soil stratigraphy which is based on soil conductivity and permittivity could be determined. Indeed, different types of soil have different properties. Figure 4 shows the extraction of soil layer based on soil velocity from the radargram.

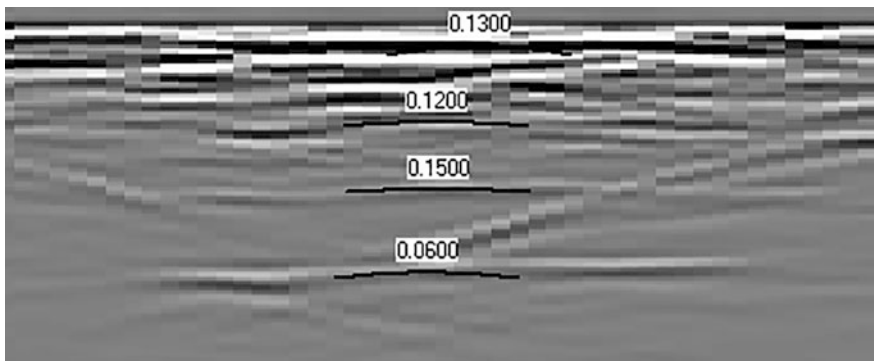


Fig. 4 Extraction of soil layer based on soil velocity

In this study, different frequencies of the GPR were used for the data acquisition. As we know, high-frequency signals would provide high resolution of radar images. As mentioned, the frequency involved in this study were 100, 250, 450, 750, and 900 MHz. The range of the frequency involved has covered both low and high frequency. As data was collected from different frequencies, a comparison of the data in terms of resolution of the data could be identified. The resolution is the depth or thickness of the soil layers.

There are different image resolutions between frequencies. The soil stratigraphy extraction was extracted from each image of different frequency, referred to the soil velocity of the radargram. After image analyses, the depths of different layers were slightly different based on their frequency. Therefore, the velocity readings of the different layers would prove the changes of soil stratigraphy. Table 1 shows the reading of soil layer depths and changes of soil velocity based on their frequency.

The signal velocity of the soil changes as the signal penetrates through different soil layers. In fact, based on Table 1, the velocity readings show that there is not much difference between the frequencies as the signal penetrates different soil layers. The outcome shows that the time gap between the construction of the test bed and the data acquisition was too long. The layers of soil were slightly mixed with the existing soils as the test bed was widely exposed to the weather conditions such as rain; thus, causing the thickness to vary in Table 1. The velocity reading for the first soil layer, which is the crusher runs stone, was almost the same for all the frequencies ranged between 0.130 and 0.135 m/ns. Despite that, from the evidence, it is proven that the soil layers have different velocity properties. The velocity reading for second and third layer similarly suits the test bed layers, which are small

**Table 1** Soil layers velocity and depth based on their frequency

Frequency (MHz)	Soil layer	Velocity (m/ns)	Depth (m)	No. of traces
100	1	0.157	1.203	29
	2	0.128	0.808	
	3	0.135	0.414	
250	1	0.150	1.188	53
	2	0.120	0.788	
	3	0.130	0.364	
400	1	0.153	1.168	60
	2	0.128	0.791	
	3	0.132	0.382	
700	1	0.161	1.250	53
	2	0.120	0.785	
	3	0.132	0.402	
900	1	0.155	1.053	92
	2	0.120	0.712	
	3	0.133	0.402	

granite stone and smooth dry sand, respectively. Both soil velocities are ranged between 0.7 and 0.8 m/ns, and between 1.0 and 1.2 m/ns, respectively.

### 3.2 Generation of 3D View Stratigraphy

From the previous results (refer Sect. 3.1), the extraction of the soil stratigraphy would help in the interpretation of generating 3D view of the soil layers. Production of this 3D view would be carried out using Reflex3D software. The 3D view of stratigraphy would give better resolution; hence, interpretation of soil layers could be made. Consequently, 3D view would better demonstrate soil stratigraphy compared to 2D stratigraphy view. Besides that, the 3D view gives the overall view of soil profile. Figure 5 shows the 3D view of soil stratigraphy.

The soil layers shown in 3D view was extracted from the 2D radargram images based on the amplitude changes. Different medium would give different reflectance amplitudes and this is how the soil layers were separated. For this 3D view, the amplitudes changes were illustrated using changes of colors. The amplitude is shown through the color bars. The negative value of amplitude gives lower amplitude reading while the positive value shows high amplitude reading.

For the extraction of the stratigraphy, different frequencies were used to study the resolution of the images. The data from the variety of GPR frequencies were used to generate the 3D view with various resolution acquisitions, which includes 100, 250, 450, 750, and 900 MHz. Figure 6 shows the 3D view of soil layers and their extraction of stratigraphy slices powered by 900 MHz frequency GPR reading.

From the figure, it is concluded that higher frequency would generate a better 3D view resolution. Hence, the 900 MHz frequency for GPR signal creates the best resolution of soil stratigraphy as the soil layers could be clearly determined by its

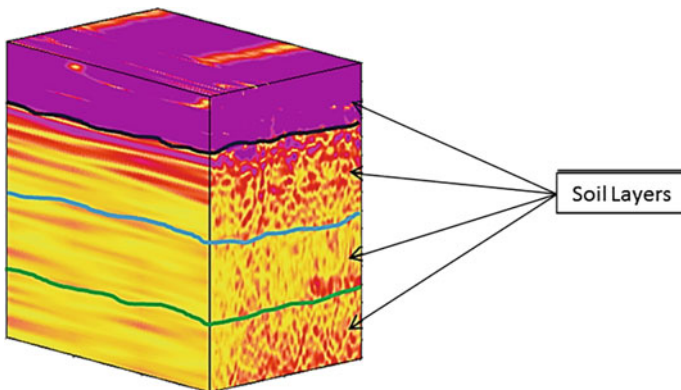
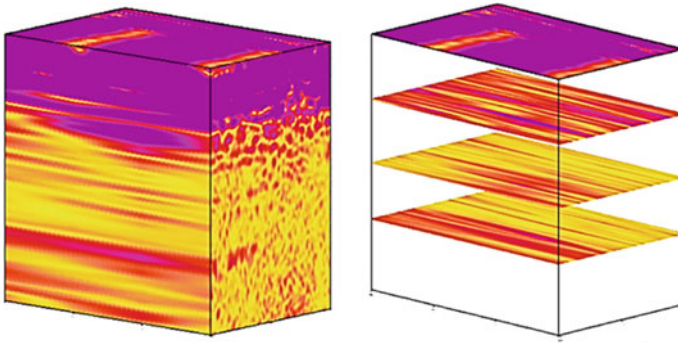


Fig. 5 The 3D view of soil stratigraphy



**Fig. 6** The 3D view of soil layers and their extraction of stratigraphy slice powered by 900 MHz frequency GPR equipment

amplitudes color changes with the visualization being sharp and clear. In conclusion, 400 MHz would give best resolution between moderate and high frequency.

### 3.3 *Real Site Stratigraphy*

Instead of the simulated test bed mentioned earlier in this chapter, this study also utilizes an actual site data in order to create a realistic soil stratigraphy. For this study, the actual site in question was located at Sungai Batu, Merbok, Kedah. The National Heritage Department (NHD) with the cooperation of several agencies had discovered a stone structure (Fig. 7) that resembles a wall which bears historical structure. The data acquisition and data processing method applied were the same as the test bed before in order to extract the soil stratigraphy. Figure 7 shows the view



**Fig. 7** The view of the actual site stratigraphy located in Sg. Batu, Merbok, Kedah



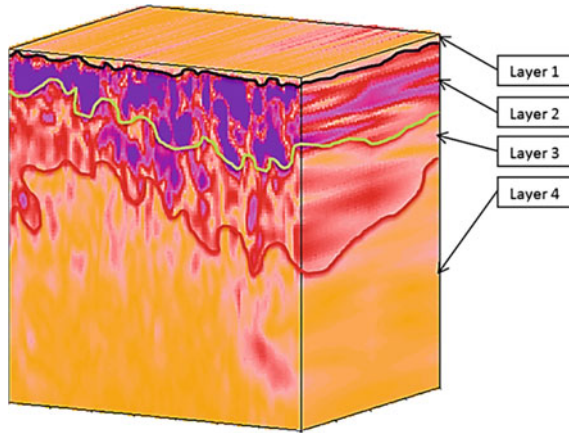


**Fig. 8** The generated 3D view with the soil stratigraphy extracted

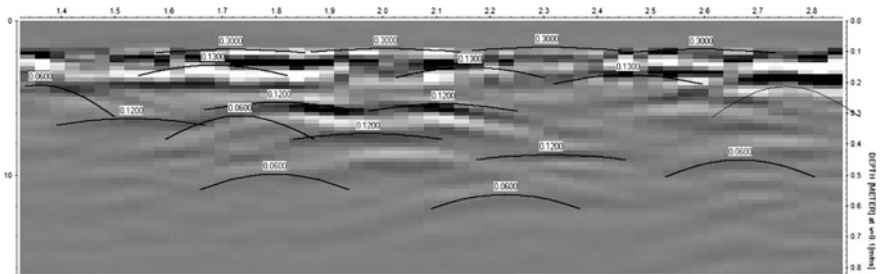


**Fig. 9** The extraction of soil velocity from radargram image

of the real stratigraphy site while Fig. 8 shows the generated 3D view from the data with the soil stratigraphy extracted.

Based on Fig. 8, there were various types of soil layers at this site. The 3D view has clearly shown that the changes in the type of soil would result in obvious changes in amplitudes color. The reading of soil velocity helped in determining the soil types. Figure 9 shows the extraction of soil velocity from radargram image, while Table 2 shows the reading of soil velocity properties.

**Table 2** Soil velocity at Merbok, Kedah

Layer	Velocity (m/ns)	Materials (m)
1	0.30	Air
2	0.12	Limestone
3	0.13	Granite
4	0.06	Clays

## 4 Conclusion

In this study, GPR has been used to produce a proper visualization for the internal structure of soil stratigraphy. With proper analysis of filtered techniques for the images, the soil stratigraphy could be interpreted and extracted. This study involved a variety of frequencies in data acquisition. The frequencies covered range between low and high frequencies of GPR, which are 100, 250, 400, 750, and 900 MHz.

From the previous section, this study has successfully identified and extracted the soil stratigraphy from the filtered radar images. The soil layers had been extracted and identified by detecting trace signals which have different reflectance for each medium.

As the test bed was constructed with the understanding of the depth of soil layers, the collected data was used to compare with the known information. From that comparison, it was determined that GPR could be used for soil stratigraphy interpretation instead of other existing equipment.

Moreover, high-frequency GPR would give the best resolution of radar images, with low penetration signal by employing the frequency from 400 to 750 MHz. Meanwhile, the low signal may penetrate deep but produces results in low resolution of the radar images. However, both low and high frequency have their pros and cons.

The 3D view of soil stratigraphy was generated based on the information and details obtained from analysis of the radar images. As shown in Fig. 6, the soil layers in 3D view mode were easier to analyse. The changes of amplitude color could be seen in this view.

The result of observation of soil stratigraphy was shown in 3D view. The soil stratigraphy is important in order to identify the medium of the ground. As discussed earlier, soil stratigraphy is not only important for the surveyors but also other users in different fields such as agriculture and construction. As a conclusion, this study is expected to help the surveyor to identify any underground utility mapping problem.

**Acknowledgements** The authors gratefully acknowledge Department of Heritage Malaysia for granting access to the investigated area and providing historical information with the help of the resident of the area and the Ministry of Higher Education, Universiti Teknologi Malaysia for their kind financial support through GUP research grant (Q.J130000.2527.11H74).

## References

1. Yang, H.W., Yang, Z.k, Pei, Y.k: Ground-penetrating radar for soil and underground pipelines using the forward modeling simulation method. *Optik—Int. J. Light Electron Opt.* **125**(23), 7075–7079 (2014)
2. Fan, C., Zhi-Yuan, W., Lei, W., Yan-Bin, W.: Application of the ground penetrating radar ARMA power spectrum estimation method to detect moisture content and compactness values in sandy loam. *J. Appl. Geophys.* **120**, 26–35 (2015)

3. Qingqing, X., Laibin, Z., Wei, L.: Acoustic detection technology for gas pipeline leakage. *Process Saf Environ.* **91**(4), 253–261 (2013)
4. Alani, A.M., Aboutaleb, M., Kilic, G.: Applications of ground penetrating radar (GPR) in bridge deck monitoring and assessment. *J. Appl. Geophys.* **97**, 45–54 (2013)
5. Abujarad, F. (ed.): Independent factor analysis for clutter reduction in GPR data for landmine detection. In: *IEEE 15th International Conference on Ground Penetrating Radar (GPR)*, 2014. Brussels, Belgium, 30 June 2014–04 July 2014
6. Clark, W.W., Burns, B.P., Ralston, J.M. (ed.): Soil effects on GPR antenna imaging quality. In: *Proceedings of SPIE 5794, Detection and Remediation Technologies for Mines and Minelike Targets X*, 968. Orlando, Florida, USA, 08 July 2005
7. Zhao, W.K., Tian, G., Wang, B.B., Shi, Z.J., Lin, J.X.: Application of 3D GPR attribute technology in archaeological investigations. *Appl. Geophys.* **9**(3), 261–269 (2012)
8. Nuzzo, L., Leucci, G., Negri, S., Carrozzo, M.T., Quarta, T.: Application of 3D visualization techniques in the analysis of GPR data for archaeology. *Ann Geophys-Italy.* **45**(2), 321–337 (2002)
9. Grasmueck, M., Weger, R., Horstmeyer, H. (eds.): Full-resolution 3D GPR imaging for geoscience and archeology. In: *10th International Conference on Ground Penetrating Radar, 2004 GPR 2004*. Delft, The Netherlands, 21–24 June 2004
10. Golebiowski, T.: 3D GPR measurements for archaeological application with interpretation aided by numerical modelling. *Acta Geophys.* **54**(4), 413–429 (2006)
11. Whiting, B.M., Hackenberger, S. (eds.): Using 3D GPR to determine the extent of possible 17th and 18th century graves beneath a concrete driveway: bridgetown Synagogue, Bridgetown, Barbados. In: *10th International Conference on Ground Penetrating Radar, 2004 GPR 2004*. Delft, The Netherlands, 21–24 June 2004
12. Novo, A., Lorenzo, H., Rial, F.I., Solla, M.: 3D GPR in forensics: finding a clandestine grave in a mountainous environment. *Forensic Sci. Int.* **204**(1–3), 134–138 (2011)
13. Almeida, E.R., Porsani, J.L., Catapano, I., Gennarelli, G., Soldovieri, F. (eds.): GPR data analysis enhanced by microwave tomography for forensic archaeology. In: *IEEE 15th International Conference on Ground Penetrating Radar (GPR)*, 2014. Brussels, Belgium, 30 June 2014–04 July 2014
14. Bradford, J.H.: Measuring water content heterogeneity using multifold GPR with reflection tomography. *Vadose Zone J.* **7**(1), 184–193 (2008)
15. Mahesh, V.S., Senthilkumar, K., Jha, P.C. (eds.): 3D digitization of sub surface features using 3D GPR. In: *ASME 2011 International Design Engineering Technical Conferences and Computers and Information in Engineering Conference*. American Society of Mechanical Engineers, Washington DC, USA, 28–30 Aug 2011
16. Widodo, W., Aditama, I.F., Syaifullah, K., Mahya Ma, J., Hidayat, M.: Detecting buried human bodies using ground-penetrating radar. *Earth Sci. Res.* **5**(2), 59 (2016)
17. Wenke, Z., Emanuele, F., Michele, P., Gang, T.: Ground penetrating radar (GPR) attribute analysis for archaeological prospection. *J. Appl. Geophys.* **97**, 107–117 (2013)
18. Igel, J., Takahashi, K., Preetz, H. (eds.): Electromagnetic soil properties and performance of GPR for landmine detection: how to measure, how to analyse and how to classify? In: *6th International Workshop on Advanced Ground Penetrating Radar (IWAGPR)*, 2011. Aachen, Germany, 22–24 June 2011
19. Akturk, O., Doyuran, V.: Integration of electrical resistivity imaging (ERI) and ground-penetrating radar (GPR) methods to identify soil profile around Necatibey Subway Station, Ankara. Turkey. *Environ. Earth Sci.* **74**(3), 2197–2208 (2015)
20. Jonard, F., Weihermüller, L., Vereecken, H., Lambot, S.: Accounting for soil surface roughness in the inversion of ultrawideband off-ground GPR signal for soil moisture retrieval. *Geophysics* **77**(1) (2012)
21. Conyers, L.B. (ed.): Moisture and soil differences as related to the spatial accuracy of GPR amplitude maps at two archaeological test sites. In: *10th International Conference on Ground Penetrating Radar, 2004 GPR 2004*. Delft, The Netherlands, 21–24 June 2004

22. Al-Qadi, I.L., Lahouar, S.: Measuring layer thicknesses with GPR—theory to practice. *Constr. Build. Mater.* **19**(10), 763–772 (2005)
23. Xu, X.L., Peng, S.P., Xiao, W., Yu, Y.: Measuring soil layer thickness in land rearrangement with GPR data. *Meas. Sci. Technol.* **25**(7) (2014)
24. Bristow, C.S. (ed.): GPR in sediments: recent advances in stratigraphic applications. In: 10th International Conference on Ground Penetrating Radar, 2004. Delft, The Netherlands, 21–24 June 2004
25. Ardekani, M.R., Druyts, P., Lambot, S., Coster, A.D., Neyt, X. (eds.): Recovering the structure of a layered soil, including layer thickness and dielectric permittivity, using the interfaces and objects backscatter detected in GPR B-scans. In: IEEE 15th International Conference on Ground Penetrating Radar (GPR), 2014. Brussels, Belgium, 30 June–4 July 2014
26. Farfán, J.N., García, E.G., Roque, D.C., Cambranis, W.K. (eds.): Integrating 20 years of geotechnical investigation using geostatistics: building a 3D model of soil stratigraphy, Campeche Bay, Gulf of Mexico. In: ASME Symposia Volumes OMAE. American Society of Mechanical Engineers, Hamburg, Germany, 4–9 June 2006
27. Beaupretre, S., Manighetti, I., Garambois, S., Malavieille, J., Dominguez, S.: Stratigraphic architecture and fault offsets of alluvial terraces at Te Marua, Wellington fault, New Zealand, revealed by pseudo-3D GPR investigation. *J. Geophys. Res.-Sol. Ea.* **118**(8), 4564–4585 (2013)
28. Conyers, L.B.: Ground-penetrating radar for landscape archaeology: method and applications. In: *Seeing the Unseen Geophysics and Landscape Archaeology*, 245–255 (2009)
29. Gaffney, V., Patterson, H., Piro, S., Goodman, D., Nishimura, Y.: Multimethodological approach to study and characterize Forum Novum (Vescovio, central Italy). *Archaeol. Prospection* **11**(4), 201–212 (2004)
30. Yalciner, C.C., Bano, M., Kadioglu, M., Karabacak, V., Meghraoui, M., Altunel, E.: New temple discovery at the archaeological site of Nysa (western Turkey) using GPR method. *J. Archaeol. Sci.* **36**(8), 1680–1689 (2009)
31. Jurg, L.: Ground-penetrating radar: a modern three-dimensional prospecting method. *Archaeol. Prospection* **10**(4), 213–240 (2003)